Los Alamos NATIONAL LABORATORY EST.1943

LA-UR-18-22117 (Accepted Manuscript)

Two-Level Transport Methods with Independent Discretization

Warsa, James S.
Anistratov, Dmitriy Yurievich

Provided by the author(s) and the Los Alamos National Laboratory (2019-06-04).

To be published in: Journal of Computational and Theoretical Transport

DOI to publisher's version: 10.1080/23324309.2018.1497991

Permalink to record: http://permalink.lanl.gov/object/view?what=info:lanl-repo/lareport/LA-UR-18-22117

Disclaimer:
Los Alamos National Laboratory, an affirmative action/equal opportunity employer, is operated by Triad National Security, LLC for the National Nuclear Security Administration of U.S. Department of Energy under contract 89233218CNA000001. By approving this article, the publisher recognizes that the U.S. Government retains nonexclusive, royalty-free license to publish or reproduce the published form of this contribution, or to allow others to do so, for U.S. Government purposes. Los Alamos National Laboratory requests that the publisher identify this article as work performed under the auspices of the U.S. Department of Energy. Los Alamos National Laboratory strongly supports academic freedom and a researcher's right to publish; as an institution, however, the Laboratory does not endorse the viewpoint of a publication or guarantee its technical correctness.

RESEARCH LIBRARY

ResearchGate

See discussions, stats, and author profiles for this publication at: https://www.researchgate.net/publication/329083131

Two-Level Transport Methods with Independent Discretization

Article · November 2018

DOI: 10.1080/23324309.2018.1497991

CITATIONS
0

READS
30

2 authors, including:

Dmitriy Y. Anistratov
North Carolina State University
56 PUBLICATIONS **204** CITATIONS

SEE PROFILE

Some of the authors of this publication are also working on these related projects:

Quasidiffusion View project

All content following this page was uploaded by Dmitriy Y. Anistratov on 05 March 2019.

The user has requested enhancement of the downloaded file.

Two-Level Transport Methods with Independent Discretization

James S. Warsa[a], Dmitriy Y. Anistratov[b]

[a]*Los Alamos National Laboratory, Los Alamos, NM, warsa@lanl.gov*
[b]*Department of Nuclear Engineering North Carolina State University Raleigh, NC, anistratov@ncsu.edu*

Abstract

In this paper we present two-level nonlinear iteration methods for the transport equation in 1D slab geometry approximated by means of the linear discontinuous finite element method (LDFEM). We develop transport schemes based on the quasidiffusion (QD) method in which the low-order QD (LOQD) equations are discretized by the linear continuous finite element method (LCFEM). This requires a mapping of the LCFEM low-order solution to the LDFEM high-order solution to define the scattering term. Several mappings are proposed and analyzed. Another proposed transport discretization scheme is based on the step characteristics for the transport equation and LCFEM for the LOQD equations. We also develop new nonlinear synthetic acceleration (NSA) methods based on the LCFEM discretization of the QD equation. To gain iterative stability, the NSA algorithms are combined with the nonlinear Krylov acceleration method. We present numerical results that demonstrate performance and basic properties of the proposed discretization schemes and iterative solution methods.

Keywords: particle transport equation, radiative transfer equation, iteration methods, finite element methods, quasidiffusion method, variable Eddington factor

1. Introduction

Discontinuous finite element methods (DFEM) are widely used for the spatial discretization of the particle transport equation [1]. This approach is intended to be an accurate and robust computational method for radiative transfer problems [2]. In this paper we develop a group of nonlinear two-level methods based on the linear discontinuous finite element method (LDFEM) discretization of the transport equation. In general, the system of equations of the class of methods being considered consists of the high-order transport equation for the angular flux and the low-order equations for angular moments of the transport solution. The high-order and low-order equations are coupled by means of (i) some factors that define exact closure relations and (ii) the scattering term in the high-order problem which is defined by the low-order solution.

Let us consider the transport equation of the following general form:

$$\mathcal{L}\psi = \mathcal{S}\psi + q\,, \tag{1}$$

where ψ is the transport solution. $\mathcal{L}$ is the operator describing steaming and collision of particles. $\mathcal{S}$ is the scattering operator. q is the external source. The low-order problem for the moments of ψ is defined by

$$\mathcal{K}(f)\mathbf{U} = Q\,, \tag{2}$$

where the solution

$$\mathbf{U} = [\phi_0, \phi_1, ...]^T \tag{3}$$

is a set of functions with fewer independent variables then ψ. The low-order problem (2) is derived by means of

- projection operators to define its operator $\mathcal{K}$,
- exact closures,
- factors or functionals $f = f(\psi)$.

The high-order problem for ψ within framework of the two-level method is given by the transport equation with a modified scattering term

$$\mathcal{L}\psi = \tilde{\mathcal{S}}(\gamma)\mathbf{U}^* + q\,, \tag{4}$$

where

$$\boldsymbol{U}^* = \mathcal{M}\mathbf{U}\,. \tag{5}$$

To formulate the high-order problem (4) we need to specify

- prolongation operator to define $\tilde{\mathcal{S}}$,
- factors or functionals $\gamma = \gamma(\psi)$,
- the mapping operator $\mathcal{M}$.

Such methods can be interpreted from several different viewpoints as projection methods, method of moments, multigrid methods, and reduction of dimensionality methods. They are known by a variety of different names as well, including nonlinear projective-iterative (NPI) methods [3], projected discrete ordinates (PDO) [4], multilevel methods [5, 6], and high-order low-order (HOLO) methods [7]. They can be applied to the solution of radiation transport, radiative transfer, multiphysics and multiscale problems, and can be used to formulate approximations for modelling other particle transport phenomena.

The first step in formulating a method of this kind is to choose the low-order problem for the moments of the angular flux. The discretizations of the high-order and low-order equations will define the essential numerical and iterative properties of the resulting nonlinear transport method. The next step in formulating such a method is to (i) identify the mapping that specifies how the discrete high-order solution is used to define closure factors and other terms for the low-order equations and (ii) identify another mapping ($\mathcal{M}$) to define how the low-order solution is used to form the scattering term in the high-order equation. As a result one obtains a nonlinear method that approximates the solution of the transport

equation. The vector of the discrete solution of such a scheme includes the discrete grid function of the angular flux and one or more angular moments of the angular flux. To study the properties and accuracy of a given scheme in this class of methods, one can use one of many approaches applied for analysis of discretization schemes for differential equations.

In this study, we consider nonlinear, two-level methods in one-dimensional slab geometry based on the quasidiffusion (QD) method [8]. The QD method is efficient for solving a wide range of particle transport and multiphysics problems [9, 10, 11]. It performs well in problems having regions of variable optical thickness, including both optically thick and thin material. The method treats problems with anisotropic scattering equally well. [3, 12, 13]. It is also known as the Variable Eddington Factor (VEF) method [14]. Various approaches have been used for spatial discretization of the low-order QD (LOQD) equations, for example, finite volume methods [3, 15, 16], finite difference methods [17], mixed finite element methods [18, 19], general finite element methods [20], linear continuous finite element methods [21], linear discontinuous finite element methods [22]. In the schemes proposed here, the LOQD equations are discretized using the linear continuous finite element method (LCFEM) applied to the second-order form of the QD equations.

The high-order transport equation is approximated by LDFEM, and the discontinuous nature of the LDFEM solution is taken into account when the QD (Eddington) factors are defined. A mapping is used that is similar to the fully-consistent mapping recently developed for the LDFEM discretization of the LOQD equations [22, 23]. The advantage in using the LCFEM LOQD equations is that the resulting linear system could be solved more efficiently then that of the LDFEM LOQD equations. The step-characteristic (SC) discretization of the high-order transport equation is also investigated.

In this paper, several methods are proposed to define the mapping of the low-order solution to the scattering term of the transport equation. One approach directly maps the LCFEM expansion of the low-order scalar flux to the LDFEM and SC discretizations of the transport equation. Another mapping is proposed for the LDFEM transport equation that approximates the slope of the scalar flux. The QD method with these mappings are second-order accurate. This is contrast to a previously developed scheme that used an LCFEM discretization of the LOQD equations and LDFEM for the transport equations but was found to be first-order accurate [21]. A third option for the LDFEM transport equation is proposed that is based on a modification of the simplified-Wareing-Larsen-Adams (SWLA) diffusion synthetic acceleration (DSA) method [24] that also appears to be first-order accurate.

We use the same LCFEM LOQD to develop nonlinear quasidiffusion synthetic acceleration (QDSA) methods to accelerate the iterative solution of LDFEM transport equation. The QDSA method is compared to DSA methods that use an LCFEM discretization of the diffusion equation in second-order form. The mappings that are used with this LCFEM diffusion equation lead to a family of nonlinear diffusion synthetic acceleration methods (NDSA). There are two cases, however, in which the mappings lead to a linear DSA scheme (one of them being the SWLA method).

The remainder of the paper is organized as follows. In Sec. 2, the QD method is formulated. In Sec. 3.1, we derive the LCFEM discretization of the LOQD and diffusion equations and define the necessary closure and cell-interface relations. In Sec 4, we present

the LDFEM transport scheme and derive several different mappings of the LCFEM low-order solution to the scattering term in the high-order LDFEM transport scheme. The SC discretization of the transport equation the corresponding low-order-solution mapping is described in Sec. 5. In Sec. 6, the two-level iteration algorithms for QD and NSA are presented. In Sec. 7, we present numerical results. We conclude with a summary in Sec. 8.

2. The QD Equations

The slab geometry transport problem with isotropic scattering is given by

$$\mu\frac{\partial\psi(x,\mu)}{\partial x}+\sigma_t(x)\psi(x,\mu)=\frac{1}{2}\sigma_s(x)\int_{-1}^{1}\psi(x,\mu')+\frac{1}{2}q(x)\,, \tag{6}$$

$$\psi(0,\mu)=\psi_{in}^{+}(\mu)\quad \text{for } \mu>0\,, \tag{7a}$$

$$\psi(X,\mu)=\psi_{in}^{-}(\mu)\quad \text{for } \mu<0\,. \tag{7b}$$

The low-order QD (LOQD) equations for the moments of the angular flux are derived by integrating the transport equation (6) over $-1\le\mu\le 1$ with weights 1 and μ. The LOQD equations are defined as [8]

$$\frac{dJ(x)}{dx}+\sigma_a\phi(x)=q\,, \tag{8a}$$

$$\frac{d}{dx}(E(x)\phi(x))+\sigma_t J(x)=0\,, \tag{8b}$$

for the scalar flux

$$\phi(x)=\int_{-1}^{1}\psi(x,\mu)d\mu \tag{9}$$

and current

$$J(x)=\int_{-1}^{1}\mu\psi(x,\mu)d\mu\,, \tag{10}$$

where the first moment equation (8b) is closed by the QD, or Eddington, factor

$$E(x)=\frac{\displaystyle\int_{-1}^{1}\mu^2\psi(x,\mu)d\mu}{\displaystyle\int_{-1}^{1}\psi(x,\mu)d\mu}\,. \tag{11}$$

The boundary conditions (BCs) for the LOQD equations (8) are defined as follows [8, 25]:

$$J(0)=C_0^{-}\left(\phi(0)-\phi_{in}^{+}\right)+J_{in}^{+}\,, \tag{12a}$$

$$J(X)=C_X^{+}\left(\phi(X)-\phi_{in}^{-}\right)+J_{in}^{-}\,, \tag{12b}$$

where the boundary factors are

$$C_0^- = \left.\frac{\int_{-1}^{0}\mu\psi(x,\mu)d\mu}{\int_{-1}^{0}\psi(x,\mu)d\mu}\right|_{x=0}, \; C_X^+ = \left.\frac{\int_{0}^{1}\mu\psi(x,\mu)d\mu}{\int_{0}^{1}\psi(x,\mu)d\mu}\right|_{x=X}, \tag{13}$$

and

$$\phi_{in}^{\pm} = \pm\int_0^{\pm1}\psi_{in}^{\pm}d\mu\,, \quad J_{in}^{\pm} = \pm\int_0^{\pm1}\mu\psi_{in}^{\pm}d\mu\,. \tag{14}$$

There exists another version of BCs for the LOQD equations, formulated by means of boundary factors that involve full-range integrals [16]. The convergence properties of the QD method with both types of BCs are similar. The high-order transport equation for the QD method is given by

$$\mu\frac{\partial\psi(x,\mu)}{\partial x} + \sigma_t\psi(x,\mu) = \frac{1}{2}\sigma_s\phi(x) + \frac{1}{2}q(x)\,. \tag{15}$$

The system of QD equations are defined by the high-order equation (15) and the LOQD equations (8).

The second-order form of the LOQD equations is derived by eliminating the current in the balance equation (8a) using the first-moment equation (8b). The second-order equation for the scalar flux are defined as

$$-\frac{d}{dx}\left(\frac{1}{\sigma_t}\frac{d(E\phi)}{dx}\right) + \sigma_a\phi = q\,. \tag{16}$$

The boundary conditions for Eq. (16) have the following form:

$$\left.\frac{d(E\phi)}{dx} + \sigma_t\Big(C_0^-\big(\phi(x) - \phi_{in}^+\big) + J_{in}^+\Big)\right|_{x=0} = 0\,, \tag{17}$$

$$\left.\frac{d(E\phi)}{dx} + \sigma_t\Big(C_X^-\big(\phi(x) - \phi_{in}^-\big) + J_{in}^-\Big)\right|_{x=X} = 0\,. \tag{18}$$

3. LCFEM Discretization

3.1. LCFEM Discretization of the LOQD Equations

To formulate the LCFEM discretization of the LOQD equations, we start from the system of unclosed equations for the moments of the angular flux

$$\frac{dJ(x)}{dx} + \sigma_a(x)\phi(x) = q(x)\,, \tag{19}$$

$$\frac{dF(x)}{dx} + \sigma_t(x)J(x) = 0\,, \tag{20}$$

where

$$F(x) = \int_{-1}^{1} \mu^2 \psi(x,\mu) d\mu \tag{21}$$

is the second angular moment. To obtain the second-order form of these moment equations we use Eq. (20) to eliminate the current in Eq. (19) and obtain

$$-\frac{d}{dx}\left(\frac{1}{\sigma_t}\frac{dF(x)}{dx}\right) + \sigma_a \phi(x) = q(x)\,. \tag{22}$$

We discretize Eq. (22) by the linear continuous finite element method. The expansion of the scalar flux is given by

$$\phi(x) = \sum_{i=0}^{N} \phi_i b_i(x)\,, \tag{23}$$

where the basis functions are

$$b_i(x) = \begin{cases} b_i^-(x) = \frac{1}{\Delta x_i}(x - x_{i-1})\,, & \text{for } x_{i-1} \le x \le x_i\,, \\ b_i^+(x) = \frac{1}{\Delta x_{i+1}}(x_{i+1} - x)\,, & \text{for } x_i \le x \le x_{i+1}\,, \end{cases} \tag{24a}$$

$$b_0(x) = \frac{1}{\Delta x_1}(x - x_0)\,, \text{ for } x_0 \le x \le x_1\,, \tag{24b}$$

$$b_N(x) = \frac{1}{\Delta x_N}(x_N - x)\,, \text{ for } x_{N-1} \le x \le x_N\,, \tag{24c}$$

$$\Delta x_i = x_i - x_{i-1}\,. \tag{25}$$

We integrate Eq. (22) with b_i $(i = 1, \ldots, N-1)$ over $x_{i-1} \le x \le x_{i+1}$

$$-\int_{x_{i-1}}^{x_{i+1}} b_i \frac{d}{dx}\left(\frac{1}{\sigma_{t,i}}\frac{dF(x)}{dx}\right) dx + \int_{x_{i-1}}^{x_{i+1}} b_i \sigma_{a,i} \phi(x) dx = \int_{x_{i-1}}^{x_{i+1}} b_i q(x) dx \tag{26}$$

to get

$$-\frac{1}{\sigma_{t,i+1}\Delta x_{i+1}}\Big(F(x_{i+1}) - F(x_i)\Big) + \frac{1}{\sigma_{t,i}\Delta x_i}\Big(F(x_i) - F(x_{i-1})\Big) + \frac{1}{6}\sigma_{a,i}\Delta x_i(2\phi_i + \phi_{i-1}) + \frac{1}{6}\sigma_{a,i+1}\Delta x_{i+1}(2\phi_i + \phi_{i+1}) = q_i^+ + q_i^-\,, \tag{27}$$

$$q_i^{\pm} = \pm \int_{x_i}^{x_{i\pm1}} b_i q(x) dx\,. \tag{28}$$

The closure for Eq. (27) is derived for the terms with the second moment F taking into account that in general the solution of the transport discretization scheme is discontinuous at cell edges. The closure for the cell-edge terms is given by

$$F(x_i) = E_i \phi_i\,, \tag{29}$$

where the cell-edge QD factor is defined by the discontinuous high-order solution as follows:

$$E_i = \left. \frac{\int_{-1}^{0} \mu^2 \psi_{i+1} d\mu + \int_{0}^{1} \mu^2 \psi_i d\mu}{\int_{-1}^{0} \psi_{i+1} d\mu + \int_{0}^{1} \psi_i d\mu} \right|_{x=x_i} \tag{30}$$

using upwinding angular flux [23]. Here $\psi_i(x,\mu)$ is the solution of a transport scheme in the i^{th} cell. If the transport solution is continuous then Eq. (30) is reduced to

$$E_i = \frac{\int_{-1}^{1} \mu^2 \psi(x_i,\mu) d\mu}{\int_{-1}^{1} \psi(x_i,\mu) d\mu} \,. \tag{31}$$

Thus, the second-order form of LOQD equations (16) discretized with LCFEM has the form

$$-\frac{1}{\sigma_{t,i+1}\Delta x_{i+1}}\Big(E_{i+1}\phi_{i+1} - E_i\phi_i\Big) + \frac{1}{\sigma_{t,i}\Delta x_i}\Big(E_i\phi_i - E_{i-1}\phi_{i-1}\Big) + \frac{1}{6}\sigma_{a,i}\Delta x_i(2\phi_i + \phi_{i-1}) + \frac{1}{6}\sigma_{a,i+1}\Delta x_{i+1}(2\phi_i + \phi_{i+1}) = q_i^+ + q_i^- \,. \tag{32}$$

To approximate the LOQD equations in the boundary cells, we integrate (20) with weights b_0 and b_N over 1^{st} and N^{th} cells, respectively, to obtain

$$-\frac{1}{\sigma_{t,1}\Delta x_1}\Big(F(x_1) - F(x_0)\Big) + \frac{1}{\sigma_{t,1}}\left.\frac{dF}{dx}\right|_{x=x_0} + \frac{1}{6}\sigma_{a,1}\Delta x_1(2\phi_0 + \phi_1) = q_0^+ \,, \tag{33}$$

$$-\frac{1}{\sigma_{t,N}}\left.\frac{dF}{dx}\right|_{x=x_N} + \frac{1}{\sigma_{t,N}\Delta x_N}\Big(F(x_N) - F(x_{N-1})\Big) + \frac{1}{6}\sigma_{a,N}\Delta x_N(2\phi_N + \phi_{N-1}) = q_N^- \,. \tag{34}$$

Using the closure (29) and Gol'din QD BCs (12) we get

$$-\frac{1}{\sigma_{t,1}\Delta x_1}\Big(E_1\phi_1 - E_0\phi_0\Big) - C_0^-\big(\phi_0 - \phi_{in}^+\big) - J_{in}^+ + \frac{1}{6}\sigma_{a,1}\Delta x_1(2\phi_0 + \phi_1) = q_0^+ \,, \tag{35}$$

$$C_X^+\big(\phi_N - \phi_{in}^-\big) + J_{in}^- + \frac{1}{\sigma_{t,N}\Delta x_N}\Big(E_N\phi_N - E_{N-1}\phi_{N-1}\Big) + \frac{1}{6}\sigma_{a,N}\Delta x_N(2\phi_N + \phi_{N-1}) = q_N^- \,. \tag{36}$$

To derive the equations for currents we integrate the first moment equation (20) over $x_{i-1} \le x \le x_{i+1}$ with the basis functions

$$\int_{x_{i-1}}^{x_{i+1}} b_i \frac{dF}{dx} dx + \int_{x_{i-1}}^{x_{i+1}} b_i \sigma_t J dx = 0 \,. \tag{37}$$

This yields

$$\frac{1}{\Delta x_{i+1}}\int_{x_i}^{x_{i+1}} F(x)dx - \frac{1}{\Delta x_i}\int_{x_{i-1}}^{x_i} F(x)dx + \int_{x_{i-1}}^{x_{i+1}} b_i\sigma_{t,i}J(x)dx = 0\,. \tag{38}$$

We now formulate the closure for the second moments in the cell as follows:

$$\int_{x_{i-1}}^{x_i} F(x)dx = \bar{E}_i\int_{x_{i-1}}^{x_i}\phi(x)dx\,, \tag{39}$$

where the cell-average QD factor is defined by

$$\bar{E}_i = \frac{\displaystyle\int_{x_{i-1}}^{x_i} dx\int_{-1}^{1} d\mu\mu^2\psi_i(x,\mu)}{\displaystyle\int_{x_{i-1}}^{x_i} dx\int_{-1}^{1} d\mu\psi_i(x,\mu)}\,. \tag{40}$$

As a result we obtain

$$\frac{1}{\Delta x_{i+1}}\bar{E}_{i+1}\int_{x_i}^{x_{i+1}}\phi(x)dx - \frac{1}{\Delta x_i}\bar{E}_i\int_{x_{i-1}}^{x_i}\phi(x)dx + \int_{x_{i-1}}^{x_{i+1}} b_i\sigma_{t,i}J(x)dx = 0\,. \tag{41}$$

We define LCFEM expansion of the current

$$J(x) = \sum_{i=0}^{N} J_i b_i(x)\,, \tag{42}$$

and substitute the expansions (23) and (42) into Eq. (41) to obtain the equations for the current

$$\frac{1}{2}\bar{E}_{i+1}(\phi_{i+1}+\phi_i) - \frac{1}{2}\bar{E}_i(\phi_i+\phi_{i-1}) + \frac{1}{6}\sigma_{t,i}\Delta x_i(2J_i+J_{i-1}) + \frac{1}{6}\sigma_{t,i+1}\Delta x_{i+1}(2J_i+J_{i+1}) = 0\,, \tag{43}$$

$$i = 1,\ldots,N-1\,.$$

The boundary conditions (12) yield

$$J_0 = C_0^-\left(\phi_o - \phi_{in}^+\right) + J_{in}^+\,, \tag{44a}$$

$$J_N = C_X^+\left(\phi_N - \phi_{in}^-\right) + J_{in}^-\,. \tag{44b}$$

3.2. LCFEM Discretization of the Diffusion Equation

The LCFEM discretization of the diffusion equation can be similarly derived from the P_1 equations

$$\frac{dJ(x)}{dx} + \sigma_a(x)\phi(x) = q(x)\,, \tag{45}$$

$$\frac{d\phi(x)}{dx} + 3\sigma_t(x)J(x) = 0\,, \tag{46}$$

written in second-order form

$$-\frac{d}{dx}\left(\frac{1}{3\sigma_t}\frac{d\phi}{dx}\right) + \sigma_a\phi(x) = q(x)\,. \tag{47}$$

Discretizing using the basis functions (24) gives

$$-\frac{1}{3\sigma_{t,i+1}\Delta x_{i+1}}\Big(\phi_{i+1} - \phi_i\Big) + \frac{1}{3\sigma_{t,i}\Delta x_i}\Big(\phi_i - \phi_{i-1}\Big) + \frac{1}{6}\sigma_{a,i+1}\Delta x_{i+1}(2\phi_i + \phi_{i+1}) = q_i^+ + q_i^-\,. \tag{48}$$

Boundary conditions can be fixed via Marshak BCs or can depend on the high-order transport solution with the Gol'din BCs used for the LOQD equations of the previous section. In the case of Marshak conditions, the equations on the boundaries are

$$-\frac{1}{3\sigma_{t,1}\Delta x_1}\Big(\phi_1 - \phi_0\Big) + \frac{1}{6}\sigma_{a,1}\Delta x_1(2\phi_0 + \phi_1) + \frac{1}{2}\phi_0 - 2J_{in}^+ = q_0^+\,, \tag{49}$$

and

$$-\frac{1}{3\sigma_{t,N}\Delta x_N}\Big(\phi_{N-1} - \phi_N\Big) + \frac{1}{6}\sigma_{a,N}\Delta x_N(2\phi_N + \phi_{N-1}) + \frac{1}{2}\phi_N + 2J_{in}^- = q_N^-\,. \tag{50}$$

With Gol'din conditions, the equations are

$$-\frac{1}{3\sigma_{t,1}\Delta x_1}\Big(\phi_1 - \phi_0\Big) + \frac{1}{6}\sigma_{a,1}\Delta x_1(2\phi_0 + \phi_1) - C_0^-\left(\phi_0 - \phi_{in}^+\right) - J_{in}^+ = q_0^+\,, \tag{51}$$

and

$$-\frac{1}{3\sigma_{t,N}\Delta x_N}\Big(\phi_{N-1} - \phi_N\Big) + \frac{1}{6}\sigma_{a,N}\Delta x_N(2\phi_N + \phi_{N-1}) + C_X^+\left(\phi_N - \phi_{in}^-\right) + J_{in}^- = q_N^+\,. \tag{52}$$

4. Linear Discontinuous FEM Transport Scheme and Formulation of Mappings

Different transport discretization schemes can be applied for solving the transport equation as a part of the two-level QD method. First, we formulate the two-level method in which (i) the transport equation is approximated by the LDFEM scheme and (ii) the LOQD equations are discretized by the developed above LCFEM scheme. Hereafter we refer to this method as LDFEM-LCFEM. The LDFEM expansion of the angular flux in the i^{th} cell is given by

$$\psi_{m,i}^{LD}(x) = \sum_{\alpha=L,R}\psi_{\alpha,m,i}b_{\alpha,i}(x)\,, \tag{53}$$

where the LDFEM basis functions are

$$b_{L,i} = \frac{1}{\Delta x_i}(x_i - x)\,, \quad b_{R,i} = \frac{1}{\Delta x_i}(x - x_{i-1})\,. \tag{54}$$

The transport LDFEM scheme has the following form:

$$\mu_m\Big(\mathbb{L}_i^b\boldsymbol{\psi}_{m,i}^b + \mathbb{L}_i\boldsymbol{\psi}_{m,i}\Big) + \sigma_{t,i}\Delta x_i\mathbb{M}_i\boldsymbol{\psi}_{m,i} = \frac{1}{2}\sigma_{s,i}\Delta x_i\mathbb{I}\tilde{\boldsymbol{\phi}}_i + \Delta x_i\mathbb{M}_i\mathbf{q}_{m,i}\,, \tag{55a}$$

where $\mathbb{I}$ is the identity matrix,

$$\mathbb{L}_i^b = \begin{bmatrix} -1 & 0 \\ 0 & 1 \end{bmatrix}, \quad \mathbb{L}_i = \frac{1}{2}\begin{bmatrix} 1 & 1 \\ -1 & -1 \end{bmatrix}, \tag{55b}$$

$$\mathbb{M}_i = \frac{1}{6}\begin{bmatrix} 2 & 1 \\ 1 & 2 \end{bmatrix}, \tag{55c}$$

$$\boldsymbol{\psi}_{m,i} = [\psi_{L,m,i}, \psi_{R,m,i}]^T\,, \tag{55d}$$

$$\boldsymbol{\psi}_{m,i}^b = [\psi_{L,m,i}^b, \psi_{R,m,i}^b]^T\,, \tag{55e}$$

$$\boldsymbol{\psi}_{L,m,i}^b \begin{cases} \psi_{in}^+(\mu_m) & \mu_m > 0,\ i = 0, \\ \psi_{R,m,i-1} & \mu_m > 0,\ i > 0, \\ \psi_{L,m,i} & \mu_m < 0, \end{cases} \tag{55f}$$

$$\boldsymbol{\psi}_{R,m,i}^b \begin{cases} \psi_{in}^-(\mu_m) & \mu_m < 0,\ i = N, \\ \psi_{L,m,i+1} & \mu_m < 0,\ i < N, \\ \psi_{R,m,i} & \mu_m > 0, \end{cases} \tag{55g}$$

and

$$\boldsymbol{q}_{m,i} = (q_{L,m,i}, q_{R,m,i})^T\,. \tag{55h}$$

The scattering term in the LDFEM transport scheme (55a) is defined by the vector of spatial moments of the scalar flux

$$\tilde{\boldsymbol{\phi}}_i = (\tilde{\phi}_{L,i}, \tilde{\phi}_{R,i})^T\,, \tag{56}$$

obtained by means of some mapping of the low-order scalar flux.

The solution of the LDFEM transport scheme (55) is used to compute the QD and boundary factors for the LOQD equations discretized by LCFEM. The QD factors (30) and (40) in the i^{th} cell are given by

$$E_i = \frac{\sum_{m^-}\mu_m^2\psi_{L,m,i+1}w_m + \sum_{m^+}\mu_m^2\psi_{R,m,i}w_m}{\sum_{m^-}\psi_{L,m,i+1}w_m + \sum_{m^+}\psi_{R,m,i}w_m}\,, \tag{57}$$

$$\bar{E}_i = \frac{\sum_m \mu_m^2\Big(\psi_{L,m,i} + \psi_{R,m,i}\Big)w_m}{\sum_m\Big(\psi_{L,m,i} + \psi_{R,m,i}\Big)w_m}\,, \tag{58}$$

where $m^\pm = \{m : \mu_m \gtrless 0\}$ and w_m is the quadrature weight.

4.1. Direct Mapping

The direct mapping is defined by the LCFEM expansion (23) and hence

$$\tilde{\phi}_{L,i} = \int_{x_{i-1}}^{x_i} b_{L,i}\tilde{\phi}_i(x)dx = \int_{x_{i-1}}^{x_i} b_{L,i}(b_{i-1}\phi_{i-1} + b_i\phi_i)dx = \int_{x_{i-1}}^{x_i} b_{L,i}(b_{i-1}^+\phi_{i-1} + b_i^-\phi_i)dx = \frac{\Delta x_i}{6}(2\phi_{i-1} + \phi_i)\,, \quad (59)$$

$$\tilde{\phi}_{R,i} = \int_{x_{i-1}}^{x_i} b_{R,i}\phi_i(x)dx = \int_{x_{i-1}}^{x_i} b_{R,i}(b_{i-1}^+\phi_{i-1} + b_i^-\phi_i)dx = \frac{\Delta x_i}{6}(\phi_{i-1} + 2\phi_i)\,. \quad (60)$$

As a result we have

$$\tilde{\boldsymbol{\phi}}_i = \mathbb{M}_i\hat{\boldsymbol{\phi}}_i\,, \quad (61)$$

where

$$\hat{\boldsymbol{\phi}}_i = (\phi_{i-1}, \phi_i)^T\,. \quad (62)$$

The LDFEM expansion of the scalar flux in the i^{th} spatial cell is the following:

$$\phi_i^{LD}(x) = \tilde{\phi}_{L,i}b_{L,i}(x) + \tilde{\phi}_{R,i}b_{R,i}(x)\,. \quad (63)$$

From Eqs. (24) and (54) we notice that

$$b_{L,i} = b_{i-1}^+\,, \quad b_{R,i} = b_i^-\,, \quad (64)$$

and, with $\phi(x)$ being the LCFEM scalar flux in (23),

$$\tilde{\phi}_{\alpha,i} = \int_{x_{i-1}}^{x_i} b_{\alpha,i}\phi(x)dx = \int_{x_{i-1}}^{x_i} b_{\alpha,i}(b_{i-1}^+\phi_{i-1} + b_i^-\phi_i)dx = \int_{x_{i-1}}^{x_i} b_{\alpha,i}(b_{L,i}\phi_{i-1} + b_{R,i}\phi_i)dx\,. \quad (65)$$

This shows that the definition of the scattering term by means of Eqs. (56)-(60) is equivalent to directly mapping the LCFEM scalar fluxes in the i^{th} spatial cell by setting

$$\tilde{\phi}_{L,i} = \phi_{i-1}\,, \quad \tilde{\phi}_{R,i} = \phi_i\,. \quad (66)$$

4.2. Linear Mapping

To compute the scattering term in the high-order LDFEM equations we approximate the scalar flux by the following linear function:

$$\tilde{\phi}_i(x) = \bar{\phi}_i^* + \frac{2}{\Delta x_i}(x - \bar{x}_i)\hat{\phi}_i^*\,, \quad x_{i-1} \le x \le x_i \quad (67)$$

and the linear mapping is given by

$$\tilde{\phi}_{L,i} = \bar{\phi}_i^* - \hat{\phi}_i^*\,, \quad \tilde{\phi}_{R,i} = \bar{\phi}_i^* + \hat{\phi}_i^*\,. \quad (68)$$

The cell-average value $\bar{\phi}_i^*$ in this mapping is defined by the LCFEM low-order solution

$$\bar{\phi}_i^* = 0.5(\phi_{i-1} + \phi_i)\,. \quad (69)$$

To derive the slope $\hat{\phi}_i^*$ we use the LDFEM discretization of the first moment LOQD equation. We integrate Eq. (8b) over the cell with LDFEM basis functions

$$\int_{x_{i-1}}^{x_i} b_{\alpha,i}\left(\frac{d}{dx}(E(x)\phi(x)) + \sigma_t J(x)\right)dx = 0\,, \quad \alpha = L, R\,. \tag{70}$$

This leads to

$$-E_{i-1}\phi(x_{i-1}) + \frac{\bar{E}_i}{\Delta x_i}\int_{x_{i-1}}^{x_i}\phi(x)dx + \sigma_{t,i}\int_{x_{i-1}}^{x_i} b_{L,i}J(x)dx = 0\,, \tag{71a}$$

$$E_i\phi(x_i) - \frac{\bar{E}_i}{\Delta x_i}\int_{x_{i-1}}^{x_i}\phi(x)dx + \sigma_{t,i}\int_{x_{i-1}}^{x_i} b_{R,i}J(x)dx = 0\,, \tag{71b}$$

Using the LDFEM expansion of the scalar flux, (63), in these expressions, along with the LDFEM expansion of the current

$$J_i^{LD}(x) = \sum_{\alpha=L,R} J_{\alpha,i}b_{\alpha,i}(x)\,, \tag{72}$$

the LDFEM discretization of Eq. (71) is

$$-E_{i-1}^b\phi^b(x_{i-1}) + \frac{1}{2}\bar{E}_i(\tilde{\phi}_{L,i} + \tilde{\phi}_{R,i}) + \sigma_{t,i}\frac{\Delta x_i}{6}\Big(2J_{L,i} + J_{R,i}\Big) = 0\,, \tag{73a}$$

$$E_i^b\phi^b(x_i) - \frac{1}{2}\bar{E}_i(\tilde{\phi}_{L,i} + \tilde{\phi}_{R,i}) + \sigma_{t,i}\frac{\Delta x_i}{6}\Big(J_{L,i} + 2J_{R,i}\Big) = 0\,. \tag{73b}$$

We now substitute Eqs. (42) and (68) into Eq. (73) to obtain

$$-E_{i-1}(\bar{\phi}_i^* - \hat{\phi}_i^*) + \bar{E}_i\bar{\phi}_i^* + \frac{1}{6}\sigma_{t,i}\Delta x_i(2J_{i-1} + J_i) = 0\,, \tag{74a}$$

$$E_i(\bar{\phi}_i^* + \hat{\phi}_i^*) - \bar{E}_i\bar{\phi}_i^* + \frac{1}{6}\sigma_{t,i}\Delta x_i(J_{i-1} + 2J_i) = 0\,. \tag{74b}$$

Then we sum Eqs. (74a) and (74b) to get

$$E_i(\bar{\phi}_i^* + \hat{\phi}_i^*) - E_{i-1}(\bar{\phi}_i^* - \hat{\phi}_i^*) + \frac{1}{2}\sigma_{t,i}\Delta x_i(J_{i-1} + J_i) = 0\,. \tag{75}$$

The equation (75) gives the definition of the slope

$$\hat{\phi}_i^* = -\frac{1}{E_i + E_{i-1}}\left((E_i - E_{i-1})\bar{\phi}_i^* + \frac{1}{2}\sigma_{t,i}\Delta x_i(J_{i-1} + J_i)\right). \tag{76}$$

In general, this linear mapping does not preserve positivity of the solution. If in a cell the slope is too large, the mapping may give a negative value of either $\tilde{\phi}_{R,i}$ or $\tilde{\phi}_{L,i}$. Various slope-limiting techniques can be applied in such a cell. Note that in Ref [19], such

reconstruction techniques are applied to a two-level method similar to ours. One way to modify the mapping in this case is to use the slope based on the LCFEM solution and define

$$\hat{\phi}_i^* = \frac{1}{2}(\phi_i - \phi_{i-1})\,. \tag{77}$$

It is equivalent to the direct mapping in this cell. If the original linear mapping produced a negative value on an iteration, then this modification should be applied in the cell during the rest of iterations. This improves robustness of the mapping and iterations.

4.3. Mapping Based on Cell Balance

The next variant of the mapping is based on approximation of cell balance using (i) the LDFEM approximation of the balance equation, (ii) the cell-edge LCFEM scalar flux, and (iii) cell-interface conditions. This mapping is a modification of the simplified-Wareing-Larsen-Adams method [24].

We apply the LDFEM discretization of the balance equation and integrate Eq. (19) with the LDFEM basis functions (54) over the i^{th} spatial cell ($x_{i-1} \le x \le x_i$) to get

$$-J^b(x_{i-1}) + \frac{1}{\Delta x_i}\int_{x_{i-1}}^{x_i} J dx + \sigma_{a,i}\frac{\Delta x_i}{6}\Big(2\phi_{L,i} + \phi_{R,i}\Big) = \frac{\Delta x_i}{6}\Big(2q_{L,i} + q_{R,i}\Big)\,, \tag{78a}$$

$$J^b(x_i) - \frac{1}{\Delta x_i}\int_{x_{i-1}}^{x_i} J dx + \sigma_{a,i}\frac{\Delta x_i}{6}\Big(\phi_{L,i} + 2\phi_{R,i}\Big) = \frac{\Delta x_i}{6}\Big(q_{L,i} + 2q_{R,i}\Big)\,, \tag{78b}$$

where $q_{\alpha,i}$, $\alpha = L, R$, are coefficients of LDFEM expansion of the source. In Eq. (78) we used LDFEM expansion of the scalar flux given by Eq. (63). $J^b(x_{i-1})$ and $J^b(x_i)$ are cell-interface currents to be defined based the solution in neighboring cells. To define these cell interface currents, we apply Gol'din cell-interface conditions (GCICs) [22, 23]. They are based on the QD BCs (12) having the form

$$J = C^-(\phi - \phi^+) + J^-\,, \tag{79a}$$

$$J = C^+(\phi - \phi^-) + J^+\,, \tag{79b}$$

where

$$\phi^\pm = \pm\int_0^{\pm 1} \psi d\mu\,, \tag{80}$$

are the partial scalar fluxes,

$$J^\pm = \pm\int_0^{\pm 1} \mu\psi d\mu \tag{81}$$

are the partial currents, and the factors are given by

$$C^\pm = \frac{\displaystyle\int_0^{\pm 1} \mu\psi d\mu}{\displaystyle\int_0^{\pm 1} \psi d\mu}\,. \tag{82}$$

It can be shown that [22, 23]

$$J^{\pm} = \frac{C^{\pm}}{C^{\pm} - C^{\mp}} \Big(J - C^{\mp} \phi \Big) \,. \tag{83}$$

Then we also note that

$$\phi = \phi^{-} + \phi^{+} = \frac{J^{-}}{C^{-}} + \frac{J^{+}}{C^{+}} \,. \tag{84}$$

This leads to

$$J^{\pm} = C^{\pm} \phi - \frac{C^{\pm}}{C^{\mp}} J^{\mp} \tag{85}$$

and hence

$$C^{\pm} C^{\mp} \phi = C^{\mp} J^{\pm} + C^{\pm} J^{\mp} \,. \tag{86}$$

Let us consider the i^{th} cell. The cell-interface current is defined by

$$J^{b} = J^{-} + J^{+} \,. \tag{87}$$

To formulate J^{b} at the left edge of the i^{th} cell ($x = x_{i-1}$), we apply J^{+} given by Eq. (85) to get

$$J^{b} = C^{+} \phi + \Big(1 - \frac{C^{+}}{C^{-}} \Big) J^{-} \,. \tag{88}$$

We use the solution in this cell

$$\psi_{i}^{LD}(x, \mu) = \sum_{\alpha = L, R} \psi_{\alpha, i}(\mu) b_{\alpha, i}(x) \tag{89}$$

to define the factors

$$C^{\pm}(x_{i-1}) = C_{L,i}^{\pm} = \frac{\displaystyle\int_{0}^{\pm 1} \mu \psi_{i,L} d\mu}{\displaystyle\int_{0}^{\pm 1} \psi_{i,L} d\mu} \,. \tag{90}$$

Then, we define the partial current J^{-} by means of Eq. (83) and the LDFEM solution in the i^{th} cell, namely, ψ_{i}^{LD} and J_{i}^{LD} (Eq. (72)). This yields

$$J^{-}(x_{i-1}) = \frac{C_{L,i}^{-}}{C_{L,i}^{-} - C_{L,i}^{+}} \Big(J_{L,i} - C_{L,i}^{+} \tilde{\phi}_{L,i} \Big) \,. \tag{91}$$

As a result we have

$$J^{b}(x_{i-1}) = C_{L,i}^{+} \phi(x_{i-1}) + J_{L,i} - C_{L,i}^{+} \tilde{\phi}_{L,i} \,. \tag{92}$$

We now define $\phi_{i}(x_{i-1})$ in Eq. (92) by the low-order LCFEM solution to obtain

$$J^{b}(x_{i-1}) = C_{L,i}^{+} \phi_{i-1} + J_{L,i} - C_{L,i}^{+} \tilde{\phi}_{L,i} \,. \tag{93}$$

Similarly, to derive J^b at the right edge of the i^{th} cell ($x = x_i$) we apply J^- defined by Eq. (85) to get

$$J^b = C^-\phi + \Big(1 - \frac{C^-}{C^+}\Big) J^+ \,. \tag{94}$$

The factors are calculated by the ψ_i^{LD} and have the form

$$C^{\pm}(x_i) = C^{\pm}_{R,i} = \frac{\displaystyle\int_0^{\pm 1} \mu\psi_{i,R} d\mu}{\displaystyle\int_0^{\pm 1} \psi_{i,R} d\mu} \,. \tag{95}$$

The equation (83) for the partial current J^+ is evaluated by the solution in the i^{th} cell

$$J^+(x_i) = \frac{C^+_{R,i}}{C^+_{R,i} - C^-_{R,i}} \Big(J_{R,i} - C^-_{R,i} \tilde{\phi}_{R,i} \Big) \,. \tag{96}$$

This yields

$$J^b(x_i) = C^-_{R,i}\phi(x_i) + J_{R,i} - C^-_{R,i}\tilde{\phi}_{R,i} \,, \tag{97}$$

where we use the low-order LCFEM solution ϕ_i to define $\phi(x_i)$. This gives rise to

$$J^b(x_i) = C^-_{R,i}\phi_i + J_{R,i} - C^-_{R,i}\tilde{\phi}_{R,i} \,. \tag{98}$$

To derive cell-local and closed system of equations for $\tilde{\phi}_{L,i}$ and $\tilde{\phi}_{R,i}$ in terms of the LCFEM solution ϕ_{i-1} and ϕ_i, we substitute Eqs. (93) and (98) into Eqs. (78) and approximate the integrals in the cell by the corresponding edge values of the currents. The mapping $\phi_{i-1}, \phi_i \to \phi_{L,i}, \phi_{R,i}$ is defined as the solution of the following cell-local equations:

$$\Big(\frac{1}{3}\sigma_{a,i}\Delta x_i + C^+_{L,i}\Big)\tilde{\phi}_{L,i} + \frac{1}{6}\sigma_{a,i}\Delta x_i \tilde{\phi}_{R,i} = C^+_{L,i}\phi_{i-1} + \frac{\Delta x_i}{6}\Big(2q_{0,L,i} + q_{0,R,i}\Big) \,, \tag{99a}$$

$$\frac{1}{6}\sigma_{a,i}\Delta x_i \tilde{\phi}_{L,i} + \Big(\frac{1}{3}\sigma_{a,i}\Delta x_i - C^-_{R,i}\Big)\tilde{\phi}_{R,i} = \frac{\Delta x_i}{6}\Big(2q_{0,L,i} + q_{0,R,i}\Big) - C^-_{R,i}\phi_i \,. \tag{99b}$$

Hereafter we refer to this method as the cell-balance mapping with GCICs.

We now formulate the mapping based on the Marshak cell-interface (MCICs) conditions that have the form

$$J = -\frac{1}{2}(\phi - \phi^+) + J^- \,, \tag{100a}$$

$$J = \frac{1}{2}(\phi - \phi^-) + J^+ \,. \tag{100b}$$

The derivation is similar to one for the mapping based on GCICs. We take into account that in Marshak conditions $C^{\pm} = \pm\frac{1}{2}$. Thus, the currents at the cell edges in the i^{th} cell are given by

$$J^b(x_{i-1}) = \frac{1}{2}\phi_{i-1} + J_{L,i} - \frac{1}{2}\tilde{\phi}_{L,i} \,, \tag{101a}$$

$$J^b(x_i) = -\frac{1}{2}\phi_i + J_{R,i} + \frac{1}{2}\tilde{\phi}_{LR,i}\,. \tag{101b}$$

The cell-balance mapping with MCICs requires the solution of the cell-local equations

$$\Big(\frac{1}{3}\sigma_{a,i}\Delta x_i + \frac{1}{2}\Big)\tilde{\phi}_{L,i} + \frac{1}{6}\sigma_{a,i}\Delta x_i\tilde{\phi}_{R,i} = \frac{1}{2}\phi_{i-1} + \frac{\Delta x_i}{6}\Big(2q_{0,L,i} + q_{0,R,i}\Big)\,, \tag{102a}$$

$$\frac{1}{6}\sigma_{a,i}\Delta x_i\tilde{\phi}_{L,i} + \Big(\frac{1}{3}\sigma_{a,i}\Delta x_i + \frac{1}{2}\Big)\tilde{\phi}_{R,i} = \frac{\Delta x_i}{6}\Big(2q_{0,L,i} + q_{0,R,i}\Big) + \frac{1}{2}\phi_i\,. \tag{102b}$$

The cell-balance mapping with MCICs uses the diffusion approximation in its formulation. This mapping is applied to formulate synthetic acceleration methods defined in terms of additive iterative corrections. These iterative algorithms are described below in Sec. 6.

5. Approximation of the Transport Equation with Step Characteristics

We consider another two-level method in which (i) the transport equation is discretized by the step characteristic (SC) scheme and (ii) the LOQD equations are approximated by the LCFEM scheme. We refer to this scheme as SC-LCFEM. The SC scheme is defined for the cell-edge ($\psi_{m,i}$) and cell-average ($\bar{\psi}_{m,i}$) angular fluxes. The SC solution is continuous at cell edges. The cell-edge and cell-average QD factors are defined as follows:

$$E_i = \frac{\sum_m \mu_m^2\psi_{m,i}w_m}{\sum_m \psi_{m,i}w_m}\,, \tag{103}$$

$$\bar{E}_i = \frac{\sum_m \mu_m^2\bar{\psi}_{m,i}w_m}{\sum_m \bar{\psi}_{m,i}w_m}\,. \tag{104}$$

The direct mapping of the LCFEM low-order QD solution that defines the cell-average scalar flux in the scattering term of the SC equations is given by

$$\bar{\phi}_i = \frac{1}{2}(\phi_{i-1} + \phi_i)\,. \tag{105}$$

6. Two-Level Iteration Methods

We describe two iterative solution algorithms that employ either discretized high-order transport equations, the LCFEM discretization of the low-order equations, and any of the mappings discussed in the previous section.

6.1. QD Method with Fixed-Point Iterations

The QD method consists of the following steps [8].

1. Solve the high-order transport problem for $\psi^{(s+1/2)}$

$$\mathcal{L}\psi^{(s+1/2)} = \mathcal{S}\tilde{\Phi}^{(s)} + q\,, \quad x \in \mathcal{A}\,, \tag{106a}$$

   where $\mathcal{A}$ is the spatial domain of the problem.
2. Calculate the LOQD factors

$$E^{(s+1/2)} = E(\psi^{(s+1/2)})\,, \quad C^{(s+1/2)} = C(\psi^{(s+1/2)})\,. \tag{106b}$$

3. Solve the LOQD equations for ϕ

$$\mathcal{K}\big(E^{(s+1/2)}\big)\phi^{(s+1)} = q\,, \quad x \in \mathcal{A} \tag{106c}$$

   with boundary conditions

$$\mathcal{B}(C^{(s+1/2)})\phi^{(s+1)} = 0\,, \quad x \in \partial\mathcal{A}\,. \tag{106d}$$

4. Map the discrete LOQD solution

$$\tilde{\Phi}^{(s+1)} = \mathcal{M}\phi^{(s+1)}\,. \tag{106e}$$

This algorithm can be viewed as a fixed-point iteration (FPI) for ϕ defined by

$$\phi^{(s+1)} = \mathrm{G}(\phi^{(s)})\,, \tag{107}$$

where G is the iterative operator.

6.2. Synthetic Acceleration Methods

The LCFEM LOQD or LCFEM diffusion equations described in the previous section can be used as part of a nonlinear synthetic acceleration (NSA) or linear diffusion synthetic acceleration (DSA) algorithm, as follows.

1. Solve the high-order transport equation for $\psi^{(s+1/2)}$

$$\mathcal{L}\psi^{(s+1/2)} = \mathcal{S}\tilde{\Phi}^{(s)}\,, \quad x \in \mathcal{A}\,, \tag{108a}$$

2. Calculate sources and boundary terms for the low-order equations

$$g^{(s+1/2)} = g(\psi^{(s+1/2)}, \psi^{(s)}) \quad \beta^{(s+1/2)} = \beta(\psi^{(s+1/2)}, \psi^{(s)}) \tag{108b}$$

3. Calculate the factors

$$E^{(s+1/2)} = E(\psi^{(s+1/2)})\,, \quad C^{(s+1/2)} = C(\psi^{(s+1/2)})\,. \tag{108c}$$

4. Solve the low-order equations for the correction $\delta\phi^{(s+1)}$

$$\mathcal{K}\big(E^{(s+1/2)}\big)\delta\phi^{(s+1)} = g^{(s+1/2)}, \quad x \in \mathcal{A}, \tag{108d}$$

$$\mathcal{B}\big(C^{(s+1/2)}\big)\delta\phi^{(s+1)} = \beta^{(s+1/2)}, \quad x \in \partial\mathcal{A}. \tag{108e}$$

5. Map the low-order solution

$$\delta\tilde{\Phi}^{(s+1)} = \mathcal{M}\delta\phi^{(s+1)}. \tag{108f}$$

6. Update

$$\tilde{\Phi}^{(s+1)} = \tilde{\Phi}^{(s)} + \delta\tilde{\Phi}^{(s+1)}. \tag{108g}$$

This two-level NSA method can be viewed as a fixed-point iteration with the iterative operator $\mathcal{H}$,

$$\phi^{(s+1)} = \mathcal{H}(\phi^{(s)}). \tag{109}$$

When the low-order equation in this algorithm is the LCFEM LOQD, this is an NSA scheme that we will refer to quasidiffusion synthetic acceleration (QDSA). When the low-order equation is LCFEM diffusion, and the algorithm includes the cell-balance mapping with GCICs and/or the Gol'din BCs for the LCFEM diffusion equation, the method is an NSA scheme that we will refer to as nonlinear diffusion synthetic acceleration (NDSA). Otherwise, when the low-order equation is LCFEM diffusion with Marshak BCs, and the cell-balance mapping with MCICs (which is the SWLA method [24]) or the direct mapping is used, it is a linear DSA method. The details of synthetic acceleration algorithms are listed in Table 1.

It is known that synthetic acceleration methods require that the spatial discretization of the low-order equations is consistent, or at least partially-consistent, with the transport discretization scheme [26]. Due to the independent discretization it is expected that the QDSA method with LCFEM discretization of the LOQD equations and the LDFEM transport discretization may have stability issues when simple, fixed-point iteration is used. Thus, nonlinear Krylov acceleration (NKA) [27] was applied to the NSA schemes to develop stable and fast convergent algorithms.

Table 1: Description of Synthetic Acceleration Methods.

Type of Method	Elements of the Method		
	Low-Order Equation	Boundary Conditions	Interface Conditions Used in Mapping
DSA	Diffusion	Marshak	Marshak
NDSA	Diffusion	Marshak	Gol'din
NDSA	Diffusion	Gol'din	Marshak
NDSA	Diffusion	Gol'din	Gol'din
QDSA	LOQD	Marshak	Marshak
QDSA	LOQD	Marshak	Gol'din
QDSA	LOQD	Gol'din	Marshak
QDSA	LOQD	Gol'din	Gol'din

7. Numerical Results

To demonstrate the performance of the proposed LDFEM-LCFEM and SC-LCFEM schemes for the discretized two-level QD method, we present mesh refinement results to examine spatial convergence. The test problem comprises the domain $x \in [0, 1]$, with $\sigma_t = 1$, $\sigma_s = 0.7$, $q = 1$, vacuum BCs and double S_5 Gauss-Legendre quadrature. The error in (i) the integral of the scalar flux over the problem domain

$$f = \int_0^1 \phi(x)dx$$

and (ii) the current at the left boundary ($J(1)$) are plotted as a function of cell width Δx. The error in the numerical solutions is compared to reference values of the LDFEM high-order transport solution calculated by means of Aitken extrapolation. Figures 1, 2, and 3 show the results of the LDFEM-LCFEM schemes with the direct, linear, and cell-balance mapping, respectively. Results for both high-order (HO) and low-order (LO) solutions are presented. The convergence behaviour of the SC-LCFEM scheme is shown in Figure 4. These results indicate that the LDFEM-LCFEM schemes with the direct and linear mapping as well as the SC-LCFEM scheme are second-order accurate, while the LDFEM-LCFEM scheme with cell-balance mapping and GCICs is first-order accurate.

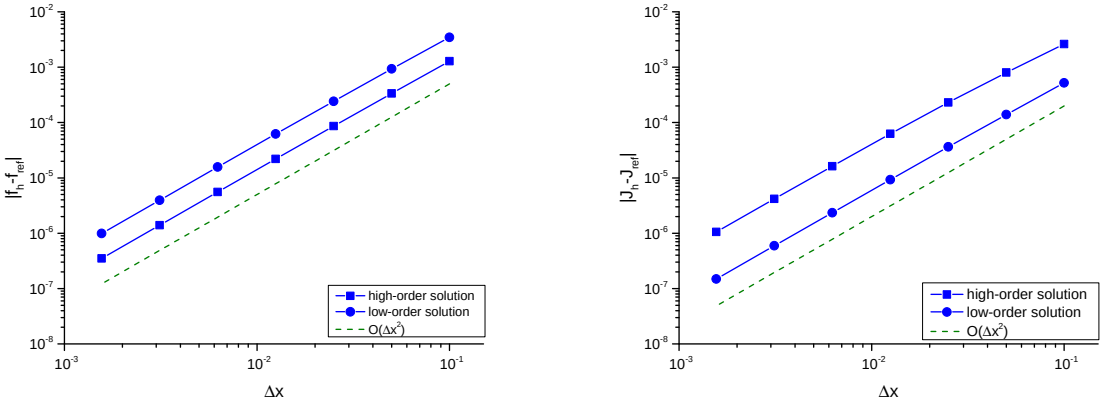

(a) $|f_h - f_{ref}|$ (b) $|J_h - J_{ref}|$

Figure 1: LDFEM-LCFEM scheme with the direct mapping. Errors in the high-order and low-order scalar fluxes and currents versus width of spatial intervals.

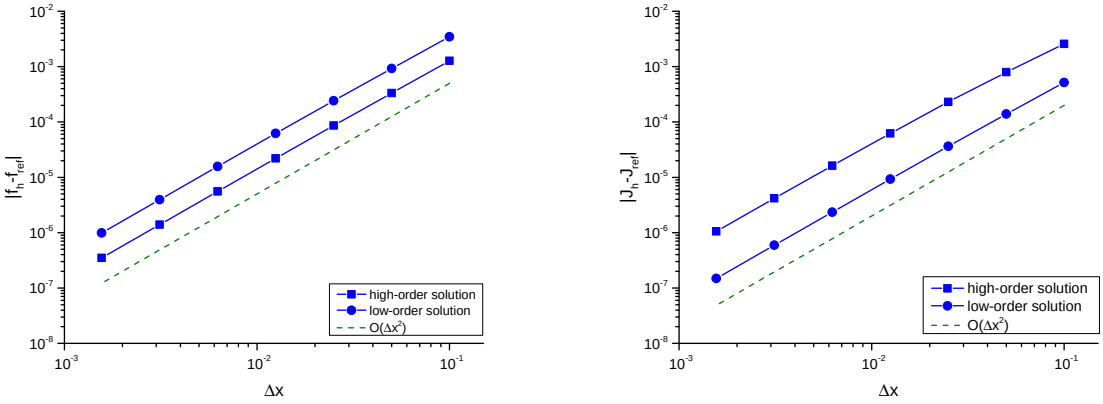

(a) $|f_h - f_{ref}|$ (b) $|J_h - J_{ref}|$

Figure 2: LDFEM-LCFEM scheme with the linear mapping. Errors in the high-order and low-order scalar fluxes and currents versus width of spatial intervals.

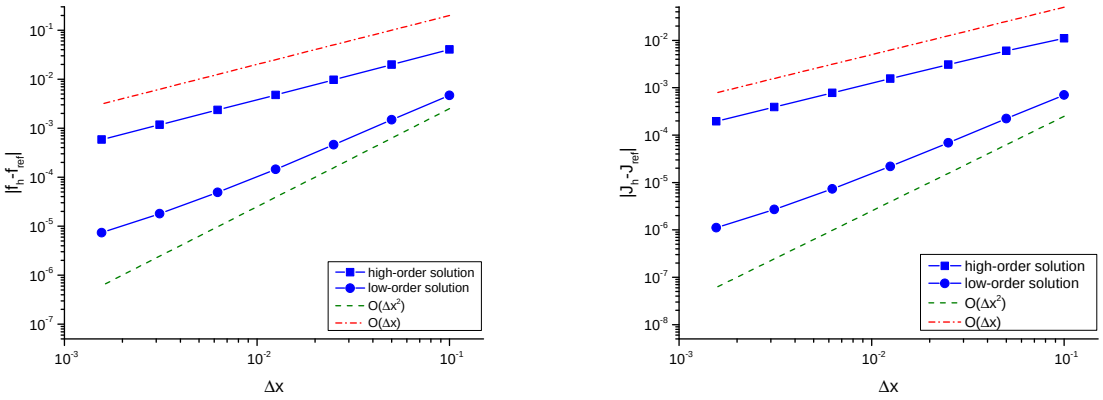

(a) $|f_h - f_{ref}|$ (b) $|J_h - J_{ref}|$

Figure 3: LDFEM-LCFEM scheme with the cell-balance mapping based on GCICs. Errors in the high-order and low-order scalar fluxes and currents versus width of spatial intervals.

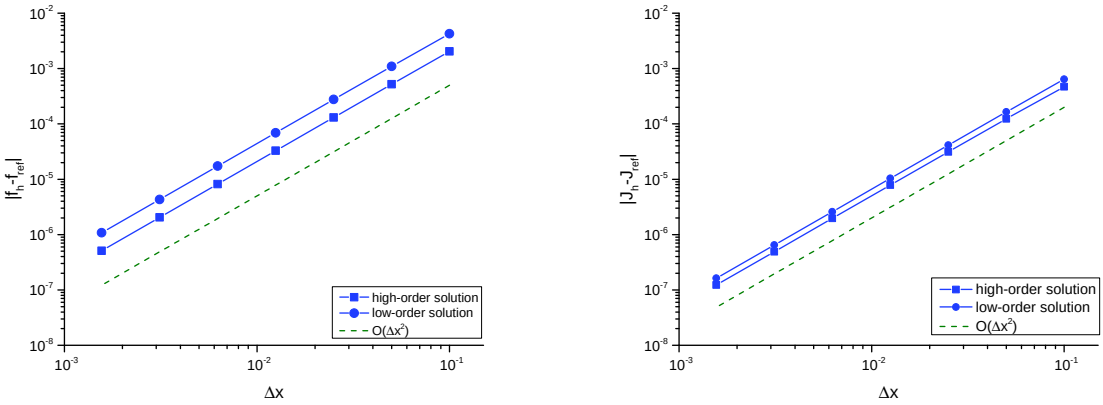

(a) $|f_h - f_{ref}|$ (b) $|J_h - J_{ref}|$

Figure 4: SC-LCFEM scheme. Errors in the high-order and low-order scalar fluxes and currents versus width of spatial intervals.

To analyze performance of the two-level methods in the thick-diffusion limit, we consider a two-region, source-free slab [28]. The left region $x \in [0, 1]$ is a pure absorber with $\sigma_t = 2$. The right region $x \in [1, 11]$ is a purely scattering material with $\sigma_t = 100$. Double S_4 Gauss-Legendre quadrature is used. There is an isotropic incoming angular flux $\psi(\mu) = 1$ on the left boundary. Figure 5 shows the numerical solutions of this diffusion-limit problem of the LDFEM-LCFEM scheme with the direct mapping and SC-LCFEM scheme. The scalar fluxes from the low-order and high-order equations are compared with the solution of the

LDFEM transport scheme on the given mesh. The results of the LDFEM-LCFEM scheme with the linear mapping are similar.

The next problem is a thick-diffusion-limit scaling test [29]. The domain $x \in [0, 1]$ is homogeneous with vacuum BCs. The cross sections and isotropic distributed source are scaled with the smallness parameter ε: $\sigma_t = \frac{1}{\varepsilon}$, $\sigma_a = \varepsilon$, $q = \varepsilon$. The spatial mesh consists of 10 equal intervals and double S_4 Gauss-Legendre quadrature is used. Figure 6 demonstrates the solutions of the test with $\varepsilon = 10^{-4}$ computed by the LDFEM-LCFEM scheme with the direct mapping and SC-LCFEM scheme, respectively. The high-order and low-order solutions of both the LDFEM-LCFEM and SC-LCFEM schemes have the asymptotic diffusion limit, even though the SC scheme itself does not. To see this, the cell-edge scalar fluxes computed with the SC scheme for $\varepsilon = 10^{-2}, 10^{-3}, 10^{-4}$ are shown in Figure 7. The amplitude of the solution is not correct and approaches zero as $\varepsilon \longrightarrow 0$. Still, the SC-LCFEM two-level QD method results in a transport method that satisfies this asymptotic limit.

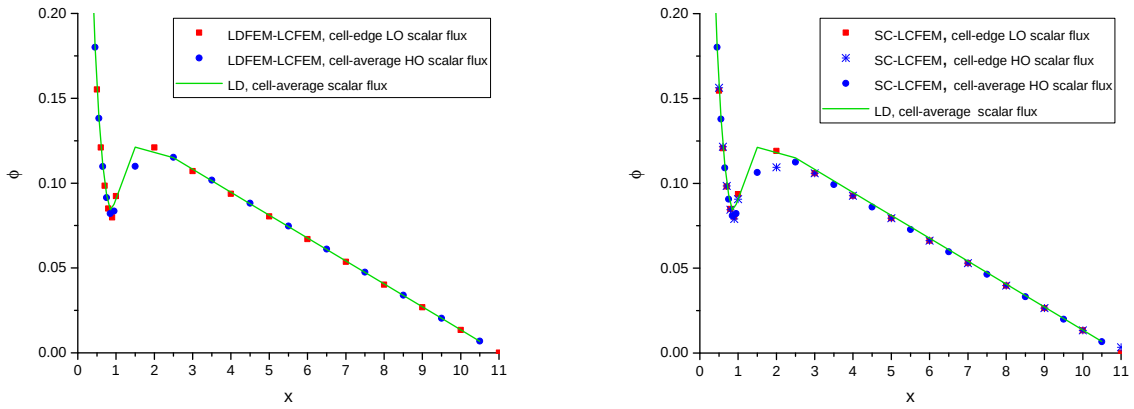

(a) LDFEM-LCFEM scheme (b) SC-LCFEM scheme

Figure 5: The two-region, thick-diffusion limit test.

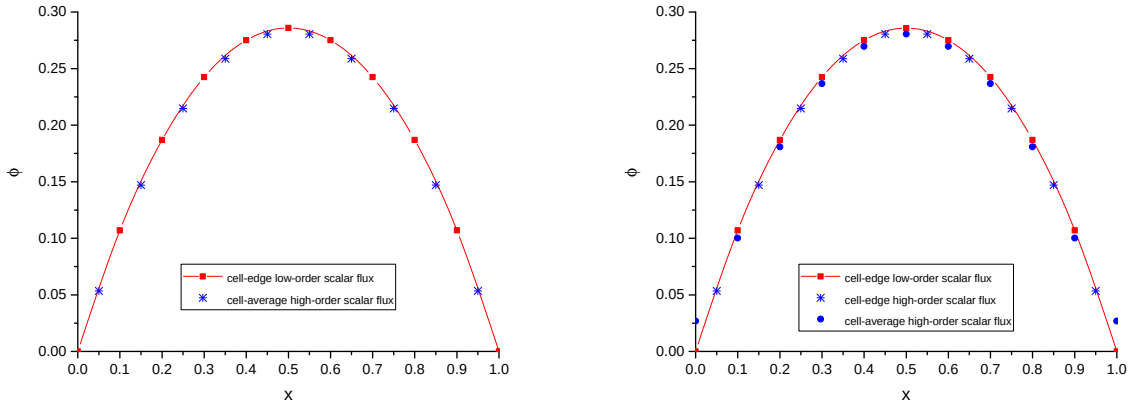

(a) LDFEM-LCFEM scheme (b) SC-LCFEM scheme

Figure 6: The diffusion-limit scaling test with $\varepsilon = 10^{-4}$.

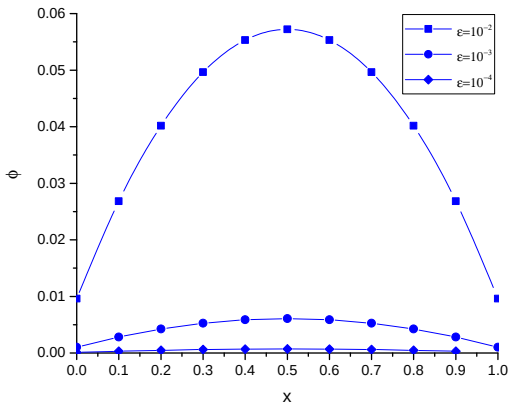

Figure 7: Solutions of the SC transport discretization in the ε diffusion-limit scaling test.

The next set of numerical results demonstrate the iterative convergence of the two-level methods. The test problem is a homogeneous slab $x \in [0, L]$ with $\sigma_t = 1$, $\sigma_s = 0.999$, $q = 1$. The left boundary is reflective and the right boundary is vacuum. To change optical thickness of the domain its width L is varied. We use uniform spatial mesh with 200 cells ($L = 200\Delta x$) and double S_4 Guass-Legendre quadrature set. The convergence criterion is

$$\| \phi^{(s)} - \phi^{(s-1)} \|_\infty < \frac{1-\rho}{\rho}\epsilon \,,$$

where s is the iteration index, $\epsilon = 10^{-8}$, and ρ is an estimate of the spectral radius. The number of iterations to achieve this convergence tolerance are tabulated for a range of

optical thickness of the spatial domain. The results of the two-level QD method are listed in Table 2. The LDFEM-LCFEM schemes with the proposed mappings and SC-LCFEM scheme converge rapidly. The number of iterations for the QDSA and NDSA methods with the cell-balance mapping are shown in Table 3 for fixed-point iteration. We present the results for the various combinations of boundary conditions and cell-interface conditions, namely, Marshak (M) and Gol'din (G) conditions (see also Table 1). As expected, the NSA fixed-point iteration can converge slowly or even fail to converge. Table 4 shows the number of iterations for the QDSA and NDSA methods with NKA(15). The NKA method provides stability and improves the rate of convergence for all the NSA methods. Note that convergence of the linear DSA schemes also improves (NKA is equivalent to GMRES [27]).

Table 2: Numbers of iterations of the QD method

	LDFEM-LCFEM			SC-LCFEM
Δx	Direct Mapping	Linear Mapping	Cell-balance Mapping with GCICs	Direct Mapping
0.01	13	13	10	12
0.05	14	14	9	14
0.1	15	15	9	14
0.5	14	14	11	12
1	13	13	13	10
2	13	13	15	8
5	12	12	15	5
10	11	12	13	3
20	10	12	10	3
50	10	10	7	3
100	8	7	5	3
1000	5	5	4	3

Table 3: Numbers of iterations for QDSA and NDSA with FPI

Method		DSA	NDSA			QDSA			
BCs		M	M	G	G	M	M	G	G
Mapping		M	G	M	G	M	G	M	G
Δx	0.01	14	14	14	14	13	13	13	13
	0.05	14	20	14	20	14	20	14	20
	0.1	13	42	13	41	13	41	13	41
	0.5	15	103	14	92	14	97	14	87
	1	20	85	20	78	20	83	20	63
	2	25	–[a]	25	–[a]	25	–[a]	25	–[a]
	5	21	57	21	49	21	56	21	48
	10	15	22	15	20	15	22	15	20
	20	12	14	12	13	12	14	12	13
	50	10	10	9	10	10	10	9	10
	100	9	9	9	9	9	9	9	9
	1000	12	12	12	12	12	12	12	12

[a] Did not converge

Table 4: Numbers of iterations for NDSA & QDSA with NKA(15)

Method		DSA	NDSA			QDSA			
BCs		M	M	G	G	M	M	G	G
Mapping		M	G	M	G	M	G	M	G
Δx	0.01	8	8	8	8	8	8	8	8
	0.05	8	11	8	10	8	11	8	11
	0.1	9	12	9	12	9	46	9	13
	0.5	10	15	10	15	10	24	10	15
	1	11	16	11	15	11	15	11	19
	2	11	13	11	14	12	13	11	13
	5	10	12	10	11	10	11	10	11
	10	9	9	9	9	9	9	9	9
	20	8	8	8	8	8	8	8	8
	50	7	7	7	7	7	7	7	7
	100	6	6	6	6	6	6	6	6
	1000	7	7	7	7	7	7	7	7

8. Conclusion

Two-level methods have been developed for solving radiation transport problems in one-dimensional slab geometry. The methods use independent discretizations of the low-order and high-order transport equations. Both QD and diffusion low-order equations are discretized with LCFEM. One of the two-level methods employs an LDFEM discretization of the transport equation. The definitions of the discrete QD (Eddington) factors and other boundary and cell-interface terms take into account the discontinuous nature of the high-order LDFEM angular flux. Several different mappings were presented of the low-order LCFEM scalar fluxes onto the LDFEM scattering source term in the transport equation. Two of these mappings yield a scheme of second-order accuracy. In another two-level method, the transport equation is discretized by SC scheme. Numerical experiments show that this scheme is a second-order accurate method and it satisfies the asymptotic diffusion limit. New NSA methods based on the QD and diffusion equations were developed. Combined with nonlinear Krylov acceleration, the NSA methods resulted in stable and fast iterative transport solution algorithms.

References

[1] R. E. Alcouffe, E. W. Larsen, W. F. Miller Jr., B. R. Wienke, Computational efficiency of numerical methods for the multigroup, discrete-ordinates neutron transport equations: The slab geometry case, Nuclear Science and Engineering 71 (2) (1979) 111–127, https://doi.org/10.13182/NSE71-111.

[2] J. E. Morel, T. A. Wareing, K. Smith, A linear-discontinuous spatial differencing scheme for S_N radiative transfer calculations, Journal of Computational Physics 128 (1996) 445– 462, https://doi.org/10.1006/jcph.1996.0223.

[3] D. Y. Anistratov, V. Ya. Gol'din, Nonlinear methods for solving particle transport problems, Transport Theory and Statistical Physics 22 (1993) 42–77, https://doi.org/10.1080/00411459308203810.

[4] E. W. Larsen, Projected discrete ordinates methods for numerical transport problems, Nuclear Science and Engineering 92 (1986) 179–185, https://doi.org/10.13182/NSE86-A18163.

[5] E. W. Larsen, Transport acceleration methods as two-level multigrid algorithms, in: W. Greenberg, J. Polewczak (Eds.), Modern mathematical methods in transport theory, Birkhauser, 1991, pp. 34–47.

[6] D. Y. Anistratov, V. Ya. Gol'din, Multilevel quasidiffusion methods for solving multigroup transport k-eigenvalue problems in one-dimensional slab geometry, Nuclear Science and Engineering 169 (2011) 111–132, https://doi.org/10.13182/NSE10-64.

[7] T. S. Haut, R. B. Lowrie, H. Park, R. M. Rauenzahn, A. B. Wollaber, A linear stability analysis of the multigroup high-order low-order (HOLO) method, in: Proc. of M&C 2015, Joint Int. Conf. on Math. and Comp. (M&C), Supercomp. in Nucl. Appl. (SNA) and the Monte Carlo (MC) Method, Nashville, TN, 2015, p. 13.

[8] V. Ya. Gol'din, A quasi-diffusion method of solving the kinetic equation, USSR Comp. Math. and Math. Phys. 4 (1964) 136–149, https://doi.org/10.1016/0041-5553(64)90085-0.

[9] E. N. Aristova, V. Ya. Gol'din, A. V. Kolpakov, Multidimensional calculations of radiation transport by nonlinear quasi-diffusion method, in: Proc. of Int. Conf. on Math. and Comp., M&C 1999, Madrid, Spain, 1999, pp. 667–676.

[10] A. Tamang, D. Y. Anistratov, A multilevel quasidiffusion method for solving space-time multigroup neutron kinetics equations coupled with the heat transfer equation, Nuclear Science and Engineering 177 (2014) 1–19, https://doi.org/10.13182/NSE13-42.

[11] L. R. Cornejo, D. Y. Anistratov, The multilevel quasidiffusion method with multigrid in energy for eigenvalue transport problem, Progress in Nuclear Energy 101 (2017) 401–408, http://dx.doi.org/10.1016/j.pnucene.2017.05.014.

[12] D. Y. Anistratov, V. Ya. Gol'din, Solution of the multigroup transport equation by the quasi-diffusion method, Preprint of the Keldysh Institute for Applied Mathematics, the USSR Academy of Sciences 128 (1986) 19 pp, in Russian.

[13] E. N. Aristova, V. Ya. Gol'din, Computation of anisotropy scattering of solar radiation in atmosphere (monoenergetic case), Journal of Quantitative Spectroscopy & Radiative Transfer 67 (2000) 139–157, https://doi.org/10.1016/S0022-4073(99)00201-0.

[14] D. Mihalas, Stellar Atmospheres, W.H. Freeman & Co, San Francisco, 1978.

[15] D. Y. Anistratov, V. Ya. Gol'din, Comparison of difference schemes for the quasi-diffusion method for solving the transport equation, Problems of Atomic Science and Engineering: Methods and Codes for Numerical Solution of Mathematical Physics Problems 2 (1986) 17–23, in Russian.

[16] M. M. Miften, E. W. Larsen, The quasi-diffusion method for solving transport problems in planar and spherical geometries, Transport Theory and Statistical Physics 22 (1993) 165–186, https://doi.org/10.1080/00411459308203811.

[17] W. A. Wieselquist, D. Y. Anistratov, J. E. Morel, A cell-local finite difference discretization of the low-order quasidiffusion equations for neutral particle transport on unstructured quadrilateral meshes, Journal of Computational Physics 273 (2014) 343–357, http://dx.doi.org/10.1016/j.jcp.2014.05.011.

[18] N. D. Vallette, Discretisation and solution of quasi-diffusion equations, Master's thesis, Texas A&M University, Nuclear Engineering, Advisor: M. L. Adams (8 2002).

[19] S. S. Olivier, J. E. Morel, Variable Eddington factor method for the S_N equations with lumped discontinuous Galerkin spatial discretization coupled to a drift-diffusion acceleration equation with mixed

finite-element discretization, Journal of Computational and Theoretical Transport 46 (6-7) (2017) 480–496, https://doi.org/10.1080/23324309.2017.1418378.
[20] E. W. Larsen, J. Yang, A functional Monte Carlo method for k-eigenvalue problems, Nuclear Science and Engineering 159 (2008) 107–126, https://doi.org/10.13182/NSE07-92.
[21] W.A.Wieselquist, A low-order quasidiffusion discretization via linear-continuous finite-elements on unstructured triangular meshes, in: Proceedings of Int. conf. PHYSOR 2010 - Advances in Reactor Physics to Power the Nuclear Renaissance, Pittsburg, PA., USA,, May 9-14, 2010.
[22] D. Y. Anistratov, J. S. Warsa, Discontinuous finite element quasidiffusion methods, Nuclear Science and Engineering 191 (2018) 105–120, https://doi.org/10.1080/00295639.2018.1450013.
[23] D. Y. Anistratov, J. S. Warsa, DFEM discretization of quasidiffusion moment equations in 1D slab geometry, in: Proceedings of M&C 2017 - International Conference on Mathematics & Computational Methods Applied to Nuclear Science & Engineering, Jeju, Korea, April 16-20, 2017.
[24] T. A. Wareing, E. W. Larsen, M. L. Adams, Diffusion accelerated discontinuous finite element schemes for the S_N equations in slab and X-Y geometries, in: Proceedings of Int. Topl. Mtg on Advances in Mathematics, Computations and Reactor Physics, Pittsburg, PA., USA,, April 29 - May 2, 1991.
[25] V. Ya. Gol'din, B. N. Chetverushkin, Methods of solving one-dimensional problems of radiation gas dynamics, USSR Comp. Math. and Math. Phys. 12 (1972) 177–189, https://doi.org/10.1016/0041-5553(72)90122-X.
[26] M. L. Adams, E. W. Larsen, Fast iterative methods for discrete-ordinates particle transport calculations, Progress in Nuclear Energy 40 (2002) 3–159, https://doi.org/10.1016/S0149-1970(01)00023-3.
[27] M. T. Calef, E. D. Fichtl, J. S. Warsa, M. Berndt, N. N. Carlson, Nonlinear Krylov acceleration applied to a discrete ordinates formulation of the k-eigenvalue problem, Journal of Computational Physics 238 (2013) 188–209, https://doi.org/10.1016/j.jcp.2012.12.024.
[28] E. W. Larsen, J. E. Morel, Asymptotic solutions of numerical transport problems in optically thick, diffusive regimes, II, Journal of Computational Physics 83 (1989) 212–236, https://doi.org/10.1016/0021-9991(89)90229-5.
[29] M. L. Adams, Discontinuous finite element transport solutions in thick diffusive problems, Nuclear Science and Engineering 137 (2001) 298–333, https://doi.org/10.13182/NSE00-41.

View publication stats